

# Derivation of Equivalent Circuit Parameters for Harmonic Operations of Surface Acoustic Wave (SAW) Interdigital Transducers (IDT's) and Reflectors

Takeshi AOKI\*      Shuzo HATTORI\*\*

Spatial harmonic properties of SAW single- and double-electrode arrays on a piezoelectric surface are described by several circuit models, by matching their circuit dispersion relations with those obtained from the field analysis in the previous papers. Their circuit parameters are expressed in terms of metallization ratio. A "mixed circuit" model is employed to overtone operations of SAW IDT and reflector consisting of each array, and a simpler "mismatched transmission-line" model to the SAW reflector only. Even harmonic operations of the single-electrode array have been theoretically found to give a strong SAW reflection and have been modeled on "shunt susceptance transmission-line" model. A brief discussion is given on mode conversion between SAW and bulk modes at the spatial harmonics of both the arrays.

## 1. Introduction

Higher harmonic operation of surface acoustic wave interdigital transducers (SAW IDT's) and reflectors allows us to extend their working frequency range beyond that of the fundamental operation limited by a photolithographic linewidth resolution<sup>1)~4)</sup>. The overtone operation of the regular (single-electrode) IDT's has been analyzed<sup>5)6)</sup>, and developed into an equivalent circuit model representation of a general case of arbitrary electrode position, gap, width and electrode polarity, while it needs numerical calculations and empirically adjustable parameters in order to include electrode field-shorting effect, or electrical loading effect<sup>7)</sup>. Since this effect influences SAW velocity and gives rise to the SAW reflection,

the above is not adequate to accurate design of the IDT having many electrodes and the SAW reflector. Recently full account has been taken of the coupling to bulk modes as well as surface modes on the IDT together with the electrical loading effect, but it needs the large amount of computer storage and time, which is inconvenient for designing SAW IDT and reflector<sup>8)</sup>. Usually a repetitively "mismatched transmission-line" model is adopted to the reflector but it also requires the empirically adjustable parameters.

In this paper we derive theoretically parameters of several simple circuit models for overtone operations of single- or double-electrode IDT's or reflectors though those fail to account for electrode end effect, mass loading effect and coupling to bulk modes.

The previous papers concern SAW propagation through the split-strip array which has a pair of sufficiently thin metal-strips with the nearest center-to-center distance  $a$  in a period  $p$ , taking account of the electrical loading

\* Associate Professor, Department of Electronics, Faculty of Engineering, Tokyo Institute of Polytechnics

\*\* Professor, Department of Electronics, Faculty of Engineering, Nagoya University.

(Received Oct. 17, 1979)

effect theoretically<sup>9),10)</sup>. When  $p$  is close to a multiple of a half-wave length  $\lambda/2$ , i. e.,  $p \simeq N\lambda$  or  $(N-1/2)\lambda$  with  $N$  being an integer, a stopband appears in SAW dispersion relation. This is a consequence of Bragg reflection due to the electrical loading effect of the strips. Since the next nearest neighbor distance is  $p-a$ , the split-strip array is reduced to a single electrode array with the periodic length  $a$  when  $p=2a$ . In the single electrode array the stopband will then occur when  $a \simeq N\lambda/2$  or  $(2N-1)\lambda/4$ . We shall apply the former case to the  $N$ -th harmonic operation of the single electrode array, and the latter to the  $(2N-1)$ -th harmonic operation of the double electrode array. The procedure to model an equivalent circuit is similar to that described in the ref. (9). A "mixed circuit" model<sup>11)</sup> can be applied to both the IDT's and the reflectors. A "mismatched transmission-line" model is suited to the reflectors only, because it is a two-port network whereas the IDT's are three-port ones. Both the models, however, do not give any stopband for the even harmonic operation of the single electrode array in contrast to the field approach predicting stopbands irrespectively of electrical connections of the electrodes<sup>10)</sup>. Consequently, the  $N$ -th harmonic operation of the single electrode array should be modeled differently according as  $N$  is odd or even.

## 2. Odd Harmonic Operation of Single Electrode Array

A single electrode array having the period  $a$  and the strip width  $w$  synchronizes with the  $N$ -th odd spatial harmonics when  $a \simeq N\lambda/2$  ( $N$ : odd). We shall assume that the array is represented by the "mixed circuit" model with a line impedance  $R_0$ , a transit angle  $\psi$  corresponding to  $a$ , the field parameter  $\bar{\alpha}$  and the

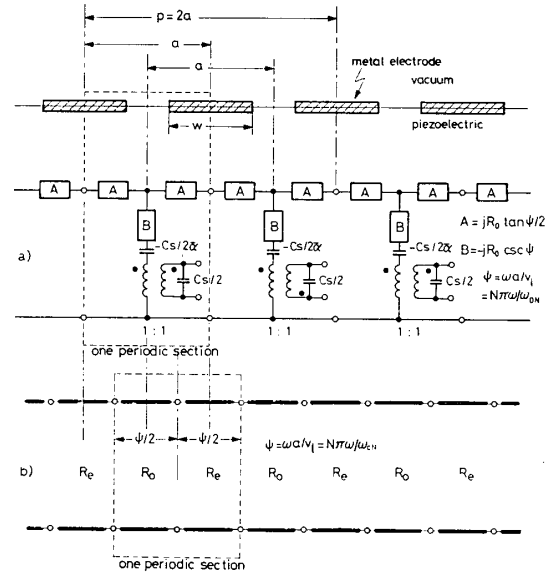


Fig. 1 Circuit models for odd harmonic operations of regular (single electrode) array; (a) "mixed circuit" model and (b) "mismatched transmission-line" model.

static electrode capacitance  $C_s$ <sup>12)</sup> as shown in Fig. 1 (a).  $\psi$  is proportional to the frequency  $\omega$  as

$$\psi = \omega a / v_l \quad (1)$$

where  $v_l$  is line velocity. It can be easily seen that shorting and disconnecting electrical ports of the equivalent circuit correspond respectively to shorted and open-circuited strip arrays. In those cases one periodic section of the circuit is reduced to a T-network, differing in shunt impedance depending on whether the strips are shorted or disconnected. The circuit dispersion relation is obtained in the same way as for the fundamental operation<sup>9)</sup>. Around at  $\omega \simeq \omega_{0N} = N\pi v_l / a$ , the wavenumber  $k$  is expressed as  $ka/2\pi = N/2 + \delta$  ( $|\delta| \ll 1$ ) with,

$$\delta \simeq \pm \frac{N}{2} \times \frac{(\omega - \omega_{0N})^{1/2} [\omega - \omega_{0N} \{1 + 4(1 - \bar{\alpha})\chi / N\pi\}]^{1/2}}{\omega_{0N}} \quad (2)$$

for the open strip array and

$$\delta \simeq \pm \frac{N}{2} \frac{(\omega - \omega_{0N})^{1/2} \{\omega - \omega_{0N} (1 - 4\bar{\alpha}\chi / N\pi)\}^{1/2}}{\omega_{0N}} \quad (3)$$

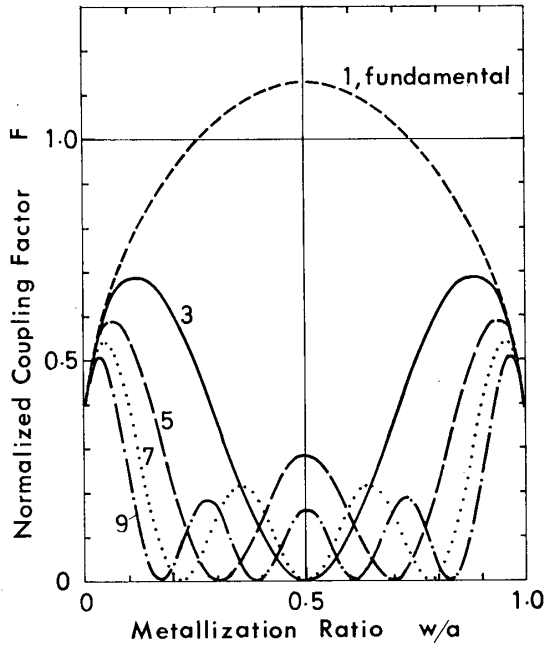
for the shorted strip array where  $\chi=2/(R_0\omega_0N C_s)$ . A stopband is found to be such a frequency range that  $\delta$  is imaginary. Meanwhile, the field analysis gives the SAW dispersion relations for both types of array;

$$\delta \simeq \pm \frac{N}{2} \left\{ \frac{(\omega - \omega_1)(\omega - \omega_2)}{\omega_1\omega_2} \right\}^{1/2} \quad (4)$$

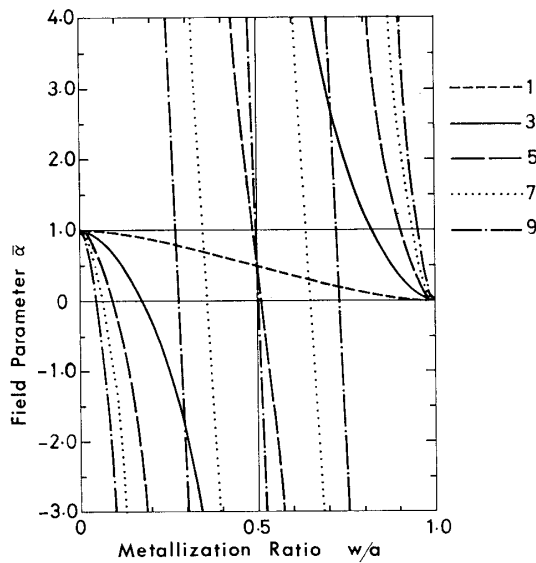
for the open strip array and

$$\delta \simeq \pm \frac{N}{2} \left\{ \frac{(\omega - \omega_1)(\omega - \omega_3)}{\omega_1\omega_3} \right\}^{1/2} \quad (5)$$

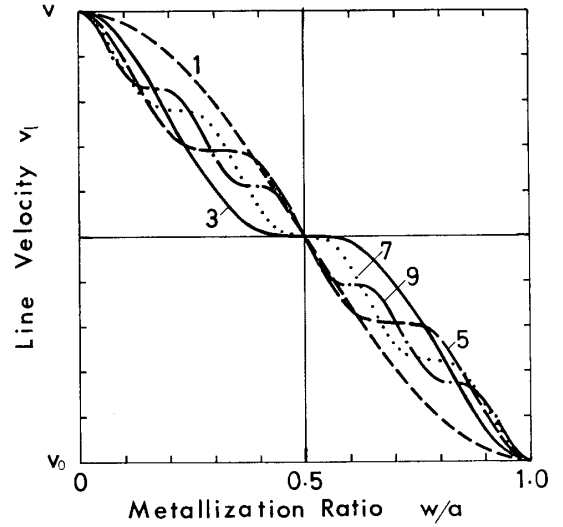
for the shorted strip array where  $\omega_1$ ,  $\omega_2$  and  $\omega_3$  are the stopband frequencies obtained from (A 36)-(A 38) in the ref. (10) if  $s=N$  and  $p=2a$  are substituted into them. Identifying the dispersion relations (4) and (5) with the circuit dispersion relations (2) and (3), respectively, we have



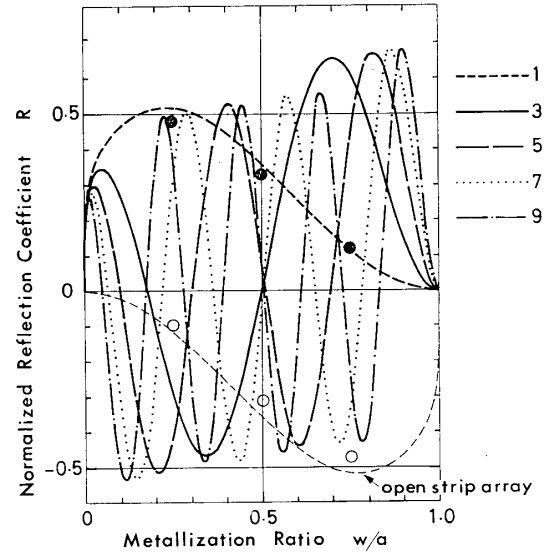
(a) Normalized coupling factor  $F$  for the the "mixed circuit" model, Fig.1 (a).



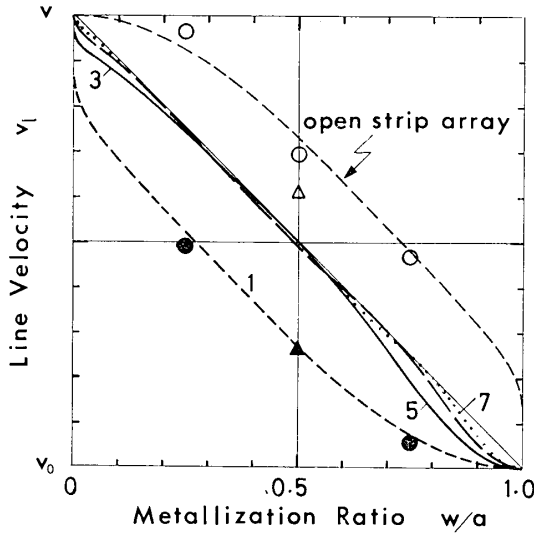
(b) Field parameter  $\alpha$  for Fig.1 (a).



(c) Line velocity for Fig.1 (a).



(d) Normalized reflection coefficient  $R$  per strip in shorted single electrode array. Experimental points are taken from the ref. (16) assuming  $K^2=0.046$ ; (●) for shorted strip array and (○) for open strip array.



(e) Line velocity  $v_l$  for the “mismatched transmission-line” model, Fig. 1 (b). Experimental points are taken from the refs. (16) (●, ○) and (19) (▲, △)

**Fig. 2** Circuit parameters and reflection coefficient per strip vs. metallization ratio  $w/a$  for the models shown in Fig. 1. The parameter is the spatial harmonic number  $N$ .

$$\left. \begin{aligned} \chi &= \frac{N\pi}{4} \frac{\omega_2 - \omega_3}{\omega_1}, \\ \bar{\alpha} &= \frac{\omega_1 - \omega_3}{\omega_2 - \omega_3}, \\ v_l &= \omega_1 a / N\pi, \quad (\omega_{0N} = \omega_1) \end{aligned} \right\} \quad (6)$$

Here we define  $F$  as a normalized  $\chi$ , i. e.,  $F = \pi\chi/K^2$ , using the SAW coupling constant  $K^2 = 2(v - v_0)/v$  for convenience, ( $v$ : the free surface Rayleigh wave velocity,  $v_0$ : the metalized surface velocity).  $F$ ,  $\bar{\alpha}$  and  $v_l$  are plotted against the metallization ratio  $w/a$  in Figs. 2 (a), (b) and (c), respectively for various harmonic number  $N$ . Apart from a numerical factor, Fig. 2 (a) is quite similar to that obtained by other workers<sup>5)~7)</sup>. The field parameter  $\bar{\alpha}$ , which indicates the proportion of the “in-line field” to the “crossed field”<sup>11)</sup>, oscillates between  $\pm\infty$  as  $w/a$  varies for every harmonic operation. When  $\bar{\alpha} = \pm\infty$ , the array doesn't work as IDT because the input electrical

impedance is purely capacitive due to  $C_s$ . When  $\bar{\alpha} = 0$ , the circuit is reduced to the “crossed field” model in which SAW regeneration can be eliminated by decreasing external electrical load<sup>13)</sup>. This is desirable to suppress SAW reflection from the IDT. For designing IDT of a given overtone, the metallization ratio  $w/a$  which makes  $F$  large and  $\bar{\alpha}$  null in Figs. 2(a) and (b) should be therefore chosen. However, rapid variation of  $\bar{\alpha}$  with  $w/a$  for large  $N$  and deviation from 1:1 mark-space ratio will increase requirement for the photolithographic linewidth resolution. Since the line velocity  $v_l$  or the synchronous frequency  $\omega_{0N}$  determines a scale of frequency axis of IDT frequency response as eq. (1) or  $\phi = N\pi\omega/\omega_{0N}$ , a precise knowledge of its deviation from  $v$  is important in narrow-band IDT design. In the limits as  $w/a \rightarrow 0$  and  $w/a \rightarrow 1$ ,  $v_l$  approaches  $v$  and  $v_0$ , respectively. In particular  $v_l = (v + v_0)/2$  at  $w/a = 0.5$  for all the harmonic operations.

The reflection coefficient for a strip is obtained from diagonal elements of the scattering matrix for the one periodic section of the circuit;  $S_{11} = S_{22} \simeq j2\bar{\alpha}\chi$  for shorted strips and  $\simeq j2(\bar{\alpha} - 1)\chi$  for open strips<sup>9)</sup>. Figure 2 (d) shows the reflection coefficient normalized by  $K^2$ ;  $R = 2\bar{\alpha}\chi/K^2 = 2\bar{\alpha}F/\pi$  versus  $w/a$  for various odd harmonic operations of the shorted strip array. The normalized reflection coefficient for the open strip array is obtained from replacing  $w/a$  by  $1 - w/a$  and changing the sign of  $R$  in Fig. 2 (d), or taking the advantage of symmetry with respect to the point ( $w/a = 0.5$ ,  $R = 0$ ) in the figure, where an example for the open case at the fundamental is given. The curves for the fundamental are similar to those of refs (14), (15), while the ref. (15) includes the electrode mass loading effect also. Dots and circles are calculated from experimental

values for YZ LiNbO<sub>3</sub> with assuming  $K^2 = 0.046^{16)}$ .

Since  $R$  decreases monotonically with  $w/a$  over the range  $0.22 < w/a < 1$  for the shorted strip array and increases over  $0 < w/a < 0.78$  for the open one, ripples of SAW resonator response can be minimized without SAW diffraction and phase distortion due to apodization<sup>4),17)</sup>, by weighting  $w/a$  within these ranges. For the  $N$ -th odd harmonic operation,  $R$  has  $N$  extrema and some of them are larger than that of the fundamental. For example,  $R \approx 0.66$  at  $w/a = 0.7$  at third harmonics of the shorted strip array, resulting in the reflection coefficient magnitude of a strip  $r = RK^2 \approx 0.030$  for YZ LiNbO<sub>3</sub>, in comparison with  $r \approx 0.0165$  at  $w/a = 0.5$  at the fundamental.

The "mixed circuit" model of which parameters  $R_0$ ,  $\bar{\alpha}$  and  $\phi$  are calculated from eq. (6) can describe the odd harmonic operations of the SAW reflector as well as those of the regular SAW IDT.

A simpler and more practical representation of the SAW reflector is the "mismatched transmission-line" model as shown in Fig. 1 (b), where one periodic section consists of cascaded two quarter-wavelength lines with the characteristic impedance  $R_e$  for the electrode region and  $R_0$  for the free surface region. Since the transmission-lines can be set equal in length ( $a/2$ ) regardless of the metallization ratio<sup>16)</sup>, we can assume that transit angle is written as  $\phi/2 = \omega a/2 v_l = N\pi\omega/2\omega_{eN}$  for each line, similarly as eq.(1). Using the Floquet's theorem for terminal voltages and currents of the circuit, we have the dispersion relation  $ka/2\pi = N/2 + \delta$  ( $|\delta| \ll 1$ ) around at  $\omega \approx \omega_{eN} = N\pi v_l/a$  with

$$\delta \approx \pm \frac{N}{4} \times \frac{\{\omega - \omega_{eN}(1 - \varepsilon/N\pi)\}^{1/2} \{\omega - \omega_{eN}(1 + \varepsilon/N\pi)\}^{1/2}}{\omega_{eN}} \quad (7)$$

where  $\varepsilon$  is related to impedance discontinuity as  $\varepsilon = R_e/R_0 - 1$ . Putting  $\omega_{eN}(1 - \varepsilon/N\pi) = \omega_1$  and  $\omega_{eN}(1 + \varepsilon/N\pi) = \omega_3$  to identify eq. (7) with eq. (5), we obtain

$$\left. \begin{aligned} \varepsilon &= -N\pi(\omega_1 - \omega_3)/2\omega_{eN} = -RK^2, \\ &= -2\bar{\alpha}\chi, \\ v_l &= (\omega_1 + \omega_3)a/2N\pi, \\ \{\omega_{eN} &= (\omega_1 + \omega_3)/2\} \end{aligned} \right\} \quad (8)$$

for the shorted strip array. For the open strip array, replacing  $\omega_3$  by  $\omega_2$ , we obtain

$$\left. \begin{aligned} \varepsilon &= -(R - 2F/\pi)K^2, \quad \{-2(\bar{\alpha} - 1)\chi\}, \\ v_l &= (\omega_1 + \omega_2)a/2N\pi, \quad \{\omega_{eN} = (\omega_1 + \omega_2)/2\} \end{aligned} \right\} \quad (9)$$

For the open strip array  $\varepsilon$  is also equal in magnitude but opposite in sign to the reflection coefficient for a strip in the array. Here identifications of stopband frequencies have been made so that the sign of  $\varepsilon$  agrees with that obtained from the experiment for the fundamental operation<sup>18)</sup>. The diagonal elements of scattering matrix are different by a factor  $-j$  between the "mixed circuit" and "mismatched transmission-line" models, because the terminal plane of the periodic section is different by  $a/4$  as can be seen from Figs. 1 (a) and (b). Since the reflective array has no electrical port, we can derive only the ratio  $R_e/R_0$  and  $\phi$ , which are sufficient for describing a reflector performance. The line velocity  $v_l$  of the "mismatched transmission-line" model for the shorted array is shown as a function of  $w/a$  in Fig. 2 (e), where  $v_l$  approaches rapidly  $v(1 - w/a) + v_0 w/a$  (the light line) as  $N$  increases. That for the open strip array can be obtained by taking the advantage of symmetry with respect to the point  $\{w/a = 0.5, v_l = (v + v_0)/2\}$  and for example of the open case,  $v_l$  for the fundamental operation is shown in Fig. 2 (e).

It can be seen from eqs. (7) ~ (9) that  $\omega_{eN}$  is the center frequency of the stopband for both types of arrays and that  $\delta$  is maximum

in magnitude but imaginary when  $\omega = \omega_{cN}$ , giving rise to the maximum reflection coefficient of the reflective arrays. At the center of the stopband, SAW phase velocity  $\omega/\text{Re}\{k\}$  is equal to  $\omega_{cN}/(N\pi/a) = v_l$ . Therefore the figure 2(e) predicts a fractional phase velocity shift at the center of the stopband as well as a scale of frequency axis of reflector response. Plots in Fig. 2(e) are the experimental values on YZ LiNbO<sub>3</sub>; the dots and circles are obtained from the ref. (16) which gives the fractional velocity shift from the phase velocity at the stopband center on the shorted strip array with  $w/a = 0.5$ , and the triangles from the ref. (19) which gives that from the free surface velocity, i. e.,  $-0.009$  for open strips and  $-0.017$  for shorted strips.

### 3. Even Harmonic Operation of Single Electrode Array

The field theory predicts a stopband independent of the electrical condition imposed on strips for a single electrode array operating at the  $N$ -th even spatial harmonics when  $a \simeq N\lambda/2$  ( $N$ : even), because  $\omega_2 = \omega_3$  at any  $w/a$  as can be seen from eqs. (A 36) ~ (A 38) in the ref. (10) if  $s = N$  (even) and  $p = 2a$  are substituted into them. This stopband has also been experimentally observed at the second harmonic<sup>20</sup>). However neither the “mixed circuit” model nor the “mismatched transmission-line” model predicts any stopband for the even harmonic operations. Since the stopband occurrence is a result of stored energy due to the electrical discontinuity between free and shorted regions on the piezoelectric surface, it is to be represented by the “shunt-susceptance transmission-line” model with a characteristic impedance  $R_0$  and a shunt susceptance  $B$  located at the center of the periodic linelength  $a$  as shown in Fig. 3<sup>20</sup>). The transit angle  $\psi$

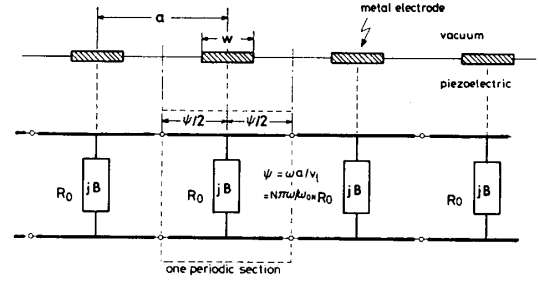


Fig. 3 “Shunt susceptance transmission-line” model for even harmonic operations of regular strip array.

is proportional to  $v_l$  as eq. (1). The dispersion relation of the repetitively connected circuits is obtained similarly as in the ref. (9);

$$\cos ka = \cos \psi - \frac{1}{2} R_0 B \sin \psi \quad (10)$$

When  $\omega \simeq \omega_{0N} = N\pi v_l/a$  and  $ka/2\pi = N/2 + \delta$  ( $|\delta| \ll 1$ ), the dispersion relation is approximated as

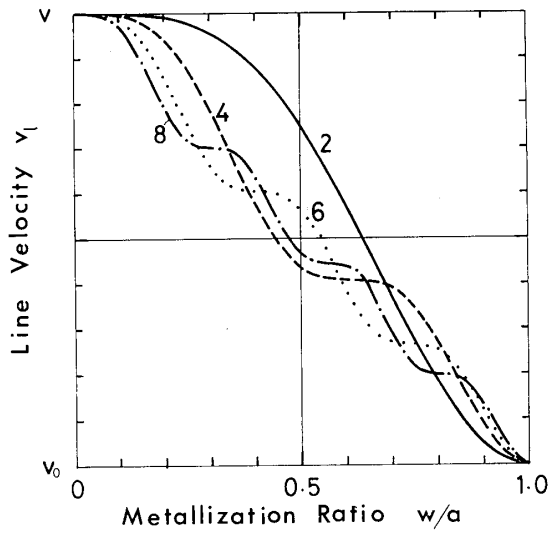
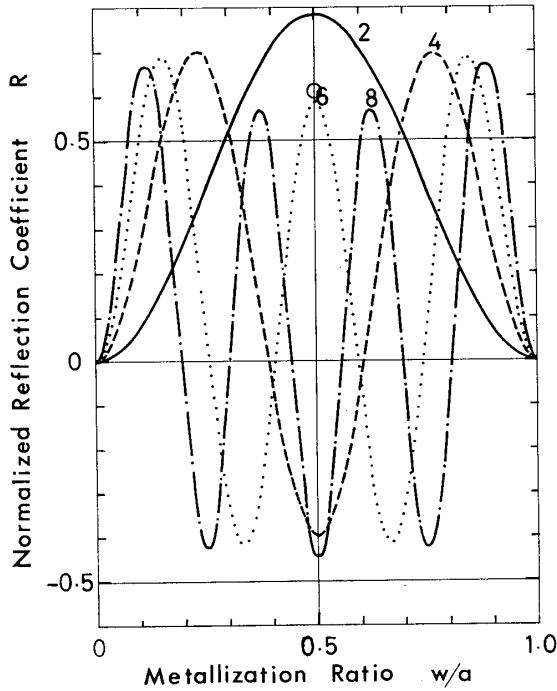
$$\delta \simeq \pm \frac{N}{2} \frac{(\omega - \omega_{0N})^{1/2} \{\omega - \omega_{0N}(1 - R_0 B/N\pi)\}^{1/2}}{\omega_{0N}} \quad (11)$$

Matching eq. (11) with eq. (4) gives unknown circuit parameters  $v_l$  and  $R_0 B$ ;

$$\left. \begin{aligned} v_l &= \omega_1 a / N\pi, \quad (\omega_{0N} = \omega_1) \\ \hat{B} &= R_0 B = N\pi(\omega_1 - \omega_2) / \omega_1 \end{aligned} \right\} \quad (12)$$

Variation of  $v_l$  with  $w/a$  is shown in Fig. 4 (a) for various values of  $N$ . Diagonal elements of the scattering matrix for a periodic section in Fig. 3 are written as  $S_{11} = S_{22} \simeq -j\hat{B}/2$  and thus the reflection coefficient magnitude of a strip  $r = \hat{B}/2$ . Figure 4(b) shows the normalized reflection coefficient  $R = \hat{B}/2 K^2$  versus  $w/a$ . For the second harmonic operation of the regular SAW reflector,  $R \simeq 0.785$  at  $w/a = 0.5$ , being larger than that of the fundamental. A numerical example calculated for YZ LiNbO<sub>3</sub> gives a reflection coefficient magnitude  $r \simeq 0.036$  whereas that obtained from the experiment gives  $r \simeq 0.028$ <sup>20</sup>). The center of the stopband giving the maximum reflection is written as

$$\omega_{cN} = (\omega_1 + \omega_2)/2 \simeq (N\pi - RK^2)v_l/a \quad (13)$$

(a) Line velocity  $v_l$ (b) Normalized reflection coefficient  $R$ . An experimental point is obtained from the ref. (20).Fig. 4 Circuit parameters vs. metallization ratio  $w/a$  for the models shown in Fig. 3. The parameter is the even spatial harmonic number  $N$ .

#### 4. Odd Harmonic Operation of Double Electrode Array

A single electrode array with a period  $a$  turns into a double electrode array with a

period  $2a$  if neighbor strips are split-connected, or connected in pairs. For this case we shall start from the "mixed circuit" model with the static capacitance of a double electrode  $C^9)$  as shown in Fig. 5 (a). Since a periodic length of the model is  $p=2a$ ,  $\psi$  is defined in this case

$$\psi = 2\omega a/v_l \quad (14)$$

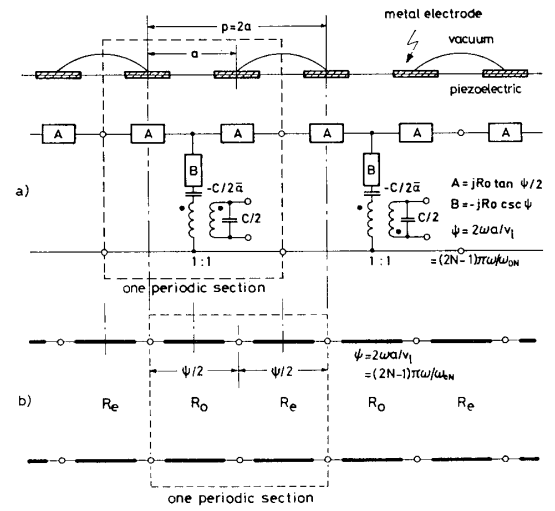


Fig. 5 Circuit models for odd harmonic operations of double electrode array; (a) "mixed circuit" model and (b) "mismatched transmission-line" model.

At the  $(2N-1)$ -th harmonic where  $\omega \simeq \omega_{0N} = (N-1/2)\pi v_l/a$ , the circuit dispersion relation is obtained from  $ka/\pi = N-1/2 + \delta$  ( $|\delta| \ll 1$ ) with

$$\delta \simeq \pm (N-1/2) (\omega - \omega_{0N})^{1/2} \times \frac{[\omega - \omega_{0N} \{1 - 2(\bar{\alpha} - 1)\chi / (N-1/2)\pi\}]^{1/2}}{\omega_{0N}} \quad (15)$$

for open double electrodes and

$$\delta \simeq \pm (N-1/2) \times \frac{(\omega - \omega_{0N})^{1/2} [\omega - \omega_{0N} \{1 - 2\bar{\alpha}\chi / (N-1/2)\pi\}]^{1/2}}{\omega_{0N}} \quad (16)$$

for shorted double electrodes where  $\chi = 2/(R_0 \omega_{0N} C)$ . The stopband frequencies  $\omega_1, \omega_2, \omega_3, \omega_4$  are estimated from eqs. (A 46)-(A 49) in

the ref. (10) where  $s=N-1/2$  and  $p=2a$  are substituted and it follows that  $\omega_1=\omega_2$  and  $\omega_3=\omega_4$ . This indicates that the stopband appears only when the double electrodes are electrically isolated<sup>10</sup>. Identifying eqs. (14) and (15) with the dispersion relations obtained from the field approach of the ref. (10);

$$\delta \simeq \pm (N-1/2) \left\{ \frac{(\omega-\omega_2)(\omega-\omega_4)}{\omega_2\omega_4} \right\}^{1/2} \quad (17)$$

for open double electrodes and

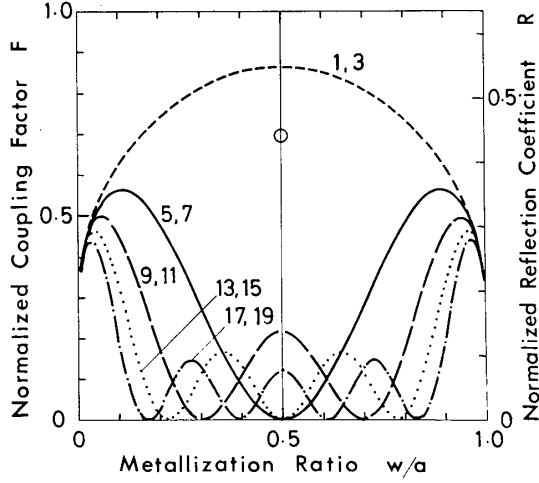
$$\delta \simeq \pm (N-1/2) \left\{ \frac{(\omega-\omega_3)(\omega-\omega_4)}{\omega_3\omega_4} \right\}^{1/2} \quad (18)$$

for shorted double electrodes, respectively, we obtain

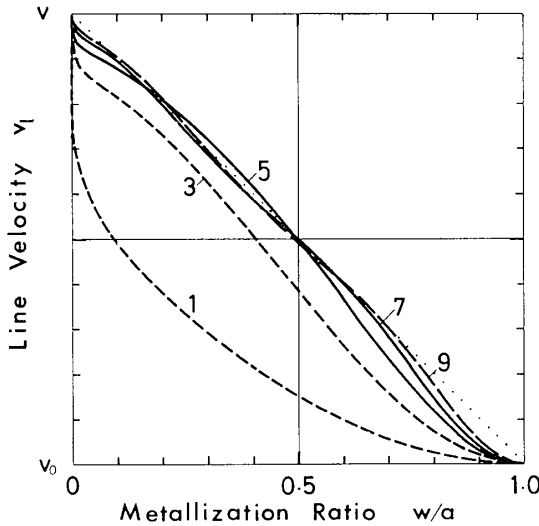
$$\left. \begin{aligned} \chi &= \frac{(N-1/2)\pi}{2} \frac{\omega_2-\omega_3}{\omega_1} \\ \bar{\alpha} &= \frac{\omega_4-\omega_3}{\omega_2-\omega_3} = 0, \\ v_l &= \omega_4 a / \{(N-1/2)\pi\}, \quad (\omega_{0N}=\omega_4). \end{aligned} \right\} \quad (19)$$

Since  $\bar{\alpha}=0$ , the equivalent circuit is reduced to the “crossed field” model, suggesting that SAW reflection from a double electrode IDT is suppressed by lowering load impedance for any overtone operation.

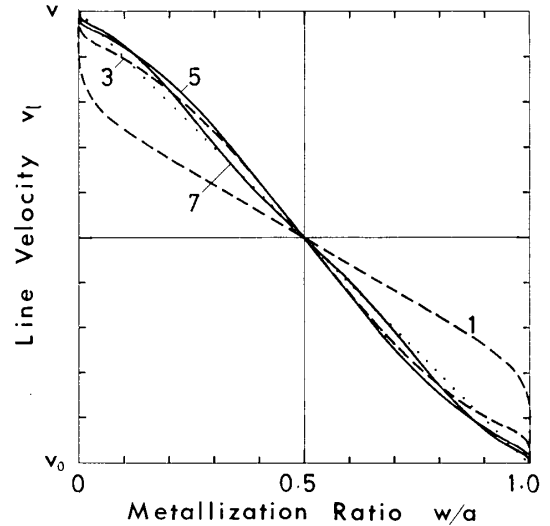
The normalized coupling factor  $F=\pi\chi/K^2$  is plotted against  $w/a$  in Fig. 6 (a) for various  $2N-1$ , which is similar to the numerical results obtained by iterative technique<sup>7</sup>). Since  $S_{11}=S_{22}\simeq -j2\chi$  for a periodic section of the open double electrode array, the reflection coefficient magnitude is proportional to  $F$ , i.e.,



(a) Normalized coupling factor  $F$  for the “mixed circuit” model, Fig. 5 (a) together with normalized reflection coefficient per open circuited double electrode  $R$ . An experimental point is taken from the ref. (21).



(b) Line velocity  $v_l$  for Fig. 5 (a).



(c) Line velocity  $v_l$  for the “mismatched transmission-line” model, Fig. 5 (b).

Fig. 6 Circuit parameters vs. metallization ratio  $w/a$  for the models shown in Fig. 5. The parameter is the odd spatial harmonic number  $2N-1$ .



$r=2FK^2/\pi$ . We show the normalized reflection coefficient  $R=2F/\pi$  in Fig. 6 (a) as well. It is worth while to be noted that  $R$  is nearly equal to 0.55 at  $w/a=0.5$  for the fundamental operation and larger than that of the single electrode array. For YZ LiNbO<sub>3</sub> the calculation gives  $r=RK^2 \simeq 0.025$  in agreement with the experimental value of 0.0204<sup>21)</sup>. Figure 6 (b) shows  $v_l$  as a function of  $w/a$ , where  $v_l$  approaches rapidly  $v(1-w/a)+v_0w/a$  (the dotted line) as  $N$  increases.

The "mismatched transmission-line" model of Fig. 5 (b) is more suited to design a double electrode SAW reflector. The impedance discontinuity  $\varepsilon=R_e/R_0-1$  and the line velocity,  $v_l$  which is related to transit angle for each section as eq. (1);  $\phi/2=\omega a/v_l=(2N-1)\pi\omega/2\omega_{cN}$ , are determined similarly as in the case of the regular SAW reflector, except that  $N$  should be replaced by  $2N-1$ ,  $\omega_1$  by  $\omega_4$  and  $a$  by  $2a$ . Accordingly, for the open double electrode array,

$$\left. \begin{aligned} \varepsilon &= -(N-1/2)\pi(\omega_4-\omega_2)/\omega_{cN} \\ &= 2FK^2/\pi = RK^2, \\ v_l &= (\omega_2+\omega_4)a/\{(2N-1)\pi\}, \\ &\quad \{\omega_{cN}=(\omega_2+\omega_4)/2\}. \end{aligned} \right\} \quad (20)$$

Again  $\omega_{cN}$ , or  $v_l$  determines the center of the stopband and is important to describing a frequency response of the reflector. The line velocity  $v_l$  is shown as a function of  $w/a$  in Fig. 6 (c).

The field analysis predicts that even harmonic operation of the double electrode array is approximated by the cases of the shorted single electrode array<sup>10)</sup>.

### 5. Possible SAW-BW Mode Conversion

Coupling between SAW and bulk wave (BW) deteriorates SAW IDT and reflector performances but sometimes it serves as a strong SAW generator. According to a simple grating

theory with ignoring crystallographic anisotropy, the coupling takes place for the harmonic operation of the strip array when

$$k_B a \sin \theta = ka + 2\pi n, \quad n = \pm 1, \pm 2, \pm 3, \dots \quad (21)$$

where  $k_B$  is the bulk wavenumber and  $\theta$  the BW incidence or transmission angle measured from the normal to the surface.

An even harmonic operation of the single electrode array where  $ka$  is close to even multiple of  $\pi$ , will cause such a mode conversion that BW direction is normal to the surface, i.e.,  $\theta=0$ , as observed in the experiment<sup>22)</sup>. This will lead to a possible explanation of the difference of reflection coefficient between the experiment and the theory at the second spatial harmonic of a single electrode array mentioned in the section 3.

At the odd spatial harmonics of the shorted double electrode array, there is no SAW reflection but SAW-BW coupling. For instance we find from eq. (21) that SAW is unidirectionally excited by a bulk wave with an incidence angle  $\sin^{-1}(v/3v_B)$ , ( $v_B$ : BW velocity) at the third spatial harmonics. This suggests an interesting possibility of a unidirectional SAW-BW convertor though a detailed estimation of the conversion efficiency requires more complicated numerical calculations including crystallographic anisotropy<sup>8),23)</sup>.

### 6. Conclusion

SAW interdigital arrays are represented by the three equivalent circuit models, i.e., "mixed circuit", "mismatched transmission-line" and "shunt susceptance transmission-line" models particularly for accurate design of harmonic operations of SAW IDT's and reflectors. Circuit parameters are determined in terms of metallization ratio by comparing the dispersion relations of the circuit models

with those obtained from the field theory. Thus obtained parameters are normalized by the SAW coupling coefficient  $K^2$  for convenience of application to any piezoelectric substrate.

The models can account for the electrical loading effect giving rise to an SAW reflection and the phase distortion around at synchronous frequency as well as the coupling strength of IDT without resorting to empirically adjustable parameters, but fail to describe the electrode end effect, mass loading effect and coupling to bulk modes.

Regular SAW IDT and regular reflector have been discussed on the basis of the “mixed circuit” model and moreover the latter has been represented by the “mismatched transmission-line” model for practical use. The “shunt-susceptance transmission-line” model

has been introduced to describe the even harmonic operation of the regular reflector where occurrence of a strong SAW reflection is theoretically confirmed.

The “mixed circuit” model has been employed to odd harmonic operation of the double electrode array and found to be always reduced to the “crossed field” model which minimizes an internal reflection with decreasing electrical load. At the fundamental and the third harmonic operations, electrically isolated double electrodes give the SAW reflection greater than that of the regular array. For the double electrode reflector, we have determined the circuit parameters of the “mismatched transmission-line” model which is more practical.

The models have been applied to previously published experiments for YZ LiNbO<sub>3</sub> with good agreement in most cases.

**Table I** Summary of circuit models for SAW IDT's and reflectors with references to analytical and numerical results.  $N$  denotes spatial harmonic number for regular strip array and  $2N-1$ , that for double electrode array.

SAW IDT & Reflector	Circuit Models & Parameters		Reference to Analytic Expressions & Numerical Calculations
Regular IDT ( $N$ : odd)	“mixed circuit” Fig. 1 (a)	$R_0 = 2\pi/(FK^2\omega_{0N}C_s)$ , ( $F = \pi\chi/K^2$ , $\omega_{0N} = N\pi v_l/a$ ), $\bar{\alpha}$ , $\psi = \omega a/v_l$	Eq. (6) & Fig. 2 (a), (b), (c)
Regular Reflector ( $N$ : odd)	Do.		Do.
	“mismatched transmission line” Fig. 1 (b)	$R_e/R_0 = 1 + \epsilon$ , $\psi = \omega a/v_l$ , shorted strip array; $\epsilon = -RK^2$ , open strip array; $\epsilon = -(R - 2F/\pi)K^2$	Eq. (8) & Fig. 2 (d), (e) Eq. (9)
Regular Reflector ( $N$ : even)	“shunt susceptance transmission line” Fig. 3	$R_0B = 2RK^2$ $\psi = \omega a/v_l$	Eq. (12) & Figs. 4 (a), (b)
Double Electrode IDT ( $2N-1$ : odd)	“mixed circuit” Fig. 5 (a)	$R_0 = 2\pi/(FK^2\omega_{0N}C)$ , ( $F = \pi\chi/K^2$ , $\omega_{0N} = (N-1/2)\pi v_l/a$ ), $\bar{\alpha} = 0$ , $\psi = 2\omega a/v_l$	Eq. (19) & Fig. 6 (a), (b)
Double Electrode Reflector ( $2N-1$ : odd)	Do.		Do.
	“mismatched transmission line” Fig. 5 (b)	$R_e/R_0 = 1 + \epsilon$ , $\epsilon = RK^2$ $\psi = 2\omega a/v_l$	Eq. (20) & Figs. 6 (a), (c)

Coupling to bulk wave at the higher spatial harmonics on these arrays has been briefly considered, with a remark suggesting a possible unidirectional SAW-BW mode conversion.

A summary of circuit parameters of the IDT's and reflectors are given in the Table I with references to analytic and numerical results.

### Acknowledgement

One of the authors, T. A. acknowledges K. A. Ingebrigtsen, Norwegian Institute of Technology, Trondheim, Norway, for valuable suggestions at early stage of this work. Numerical calculations were made at Nagoya University Computation Center.

### References

- 1) WEGLEIN, R. D., and NUDD, G. R., "Space-harmonic response of surface surface wave transducers", 1972 *Ultrasonics Symposium Proceedings*, IEEE Cat. 72 CHO 708-8 SU, pp. 346-352.
- 2) KERBEL, S. J., "Design of harmonic surface acoustic wave (SAW) oscillators without external filtering and new data on the temperature coefficient of quartz", 1974 *Ultrasonics Symposium Proceedings*, IEEE Cat. 74 CHO 896-1 SU, pp. 276-281.
- 3) HAYDL, W. H., "Precision narrowband surface wave band pass filters", *ibid.*, pp. 429-432.
- 4) LAKIN, K. M., and JOSEPH, T. R., "Surface wave resonators", 1975 *Ultrasonics Symposium Proceedings*, IEEE Cat. 75 CHO 994-4 SU, pp. 269-278.
- 5) BAHR, A. J., and LEE, R. E., "Equivalent-circuit model for interdigital transducers with varying electrode width", *Elect. Lett.*, **9**, 13, pp. 281-282, (June 1973).
- 6) AULD, B. A., and KINO, G. S., "Normal mode theory for acoustic waves and its application to the interdigital transducer", *IEEE Trans.*, *ED-18*, 10, pp. 898-908, (Oct. 1971).
- 7) SMITH, W. R., and PEDLER, W. F., "Fundamental-and harmonic-frequency circuit-model analysis of interdigital transducers with arbitrary metallization ratios and polarity sequences", *IEEE Trans.*, *MTT-23*, 11, pp. 853-869, (Nov. 1975).
- 8) MILSOM, R. F., RELLY, N. H. C., and REDWOOD, M., "Analysis of generation and detection of surface and bulk acoustic waves by interdigital transducers", *IEEE Trans.*, *SU-24*, 3, pp. 147-166, (May 1977).
- 9) AOKI, T., and INGEBRIGTSEN, K. A., "Equivalent circuit parameters of interdigital transducers derived from dispersion relations for surface acoustic waves in periodic metal gratings", *ibid.*, pp. 167-178.
- 10) AOKI, T., and INGEBRIGTSEN, K. A., "Acoustic surface waves in split-strip periodic metal gratings on a piezoelectric surface", *ibid.*, pp. 179-193.
- 11) MILSOM, R. F., and REDWOOD, M., "Interdigital piezoelectric Rayleigh wave transducer: An improved equivalent circuit", *Elect. Lett.*, **7**, 9, pp. 217-218, (May 1971).
- 12) ENGAN, H., "Excitation of elastic surface waves by spatial harmonics of interdigital transducers", *IEEE Trans.*, *ED-16*, 12, pp. 1014-1017, (Dec. 1969).
- 13) SMITH, W. R., "Experimental distinction between crossed-field and in-line three-port circuit models for interdigital transducers", *IEEE Trans.*, *MTT-22*, 11, pp. 960-964, (Nov. 1974).
- 14) EMTAGE, P. R., "Description of interdigital transducers", *J. Appl. Phys.*, **43**, 11, pp. 4486-4489, (Nov. 1972).
- 15) SUZUKI, Y., SHIMIZU, H., TAKEUCHI, M., NAKAMURA, K., and YAMADA, A., "Some studies on SAW resonators and multiple-mode filters", 1976 *Ultrasonics Symposium Proceedings*, IEEE Cat., 76 CH 1120-5 SU, pp. 297-302.
- 16) MATTHAEI, G. L., BARMAN, F., and SAVAGE, E. B., "SAW reflecting arrays", *Elect. Lett.*, **12**, 21, pp. 556-557, (Sep. 1976).
- 17) TANCRESS, R. H., and WILLIAMSON, R. C., "Wavefront distortion of acoustic surface waves from apodized interdigital transducers", *Appl. Phys. Lett.*, **19**, 11, pp. 456-459, (Dec. 1971).
- 18) MATTHAEI, G. L., O'SHAUGHNESSY, B. P., and BARMAN, F., "Relations for analysis and

- design of surfacewave resonators", *IEEE Trans.*, *SU-23*, 2, pp. 99-107, (March. 1976).
- 19) WILLIAMSON, R. C., "Measurement of the propagation characteristics of surface and bulk waves in  $\text{LiNbO}_3$ ", 1972 *Ultrasonics Symposium Proceedings* IEEE Cat. 72 CHO 708-8 SU, pp. 323-327.
- 20) LI, R. C. M., and MELNGAILIS, J., "The influence of stored energy at step discontinuities on the behavior of surface-wave gratings", *IEEE Trans.*, *SU-22*, 3, pp. 189-198, (May. 1975).
- 21) HAYDL, W. H., DISCHLER, B., and HIESINGER, P., "Multimode SAW resonators-A method to study the optimum resonator design", 1976 *Ultrasonics Symposium Proceedings*, IEEE Cat. 76 CHO 1120-5 SU, pp. 287-296.
- 22) BERTONI, H. L., "Piezoelectric Rayleigh wave excitation by bulk wave scattering", *IEEE Trans.*, *MTT-17*, 11, pp. 873-882, (Nov. 1969).
- 23) WAGERS, R. S., "Plate mode coupling in acoustic surface devices", *IEEE Trans.*, *SU-23*, 2, pp. 113-127, (March. 1976).